On page 27, please delete the paragraph beginning on line 3, and substitute therefor:

V,

FIG. 95 depicts cumulative condensable hydrocarbons as a function of temperature produced by heating a coal cube.

On page 27, please delete the three paragraphs beginning on line 19, and substitute therefor:

K2

FIG. 106 depicts percentage ethene to ethane produced from a coal formation as a function of heating rate in a laboratory test;

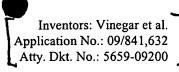
FIG. 107 depicts product quality of fluids produced from a coal formation as a function of heating rate in a laboratory test;

FIG. 108 depicts weight percentages of various fluids produced from a coal formation for various heating rates in a laboratory test;

On page 61, please delete the paragraph beginning on line 4, and substitute therefor:

<mark>የ</mark>ን

FIG. 9 illustrates an embodiment of unit cell 404. Unit cell 404 includes heat sources 400 and production wells 402. Unit cell 404 may have six full heat sources 400a and six partial heat sources 400b. Full heat sources 400a may be closer to production well 402 than partial heat sources 400b. In addition, an entirety of each of the full heat sources 400a may be located within unit cell 404. Partial heat sources 400b may be partially disposed within unit cell 404. Only a portion of heat source 400b disposed within unit cell 404 may be configured to provide heat to a portion of a coal formation disposed within unit cell 404. A remaining portion of heat source 400b disposed outside of unit cell 404 may be configured to provide heat to a remaining portion of the coal formation outside of unit cell 404. Therefore, to determine a number of heat sources within unit cell 404 partial heat source 400b may be counted as one-half of full heat



43

source 400a. In other unit cell embodiments, fractions other than 1/2 (e.g., 1/3) may more accurately describe the amount of heat applied to a portion from a partial heat source.

On page 96, please delete the paragraph beginning on line 1, and substitute therefor:

ħα

FIG. 23a illustrates a cross-sectional view of an embodiment of a centralizer 581 disposed on conductor 580. FIG. 23b illustrates a perspective view of the embodiment shown in FIG. 23a. Centralizer 581 may be made of any suitable electrically insulating material that may substantially withstand high voltage at high temperatures. Examples of such materials may be aluminum oxide and/or Macor. Discs 581d may maintain positions of centralizer 581 relative to conductor 580. Discs 581d may be metal discs welded to conductor 580. Discs 581d may be tack-welded to conductor 580. Centralizer 581 may substantially electrically insulate conductor 580 from conduit 582.

On page 108, please delete the paragraph beginning on line 15, and substitute therefor:

Ą۶

Oxidizing fluid 623 may mix with fuel fluid 621 in the oxidation region of inner conduit 638. Either oxidizing fluid 623 or fuel fluid 621, or a combination of both, may be preheated external to the combustor to a temperature sufficient to support oxidation of fuel fluid 621. Oxidation of fuel fluid 621 may provide heat generation within outer conduit 636. The generated heat may provide heat to at least a portion of a coal formation proximate to the oxidation region of inner conduit 638. Products 625 from oxidation of fuel fluid 621 may be removed through outer conduit 636 outside inner conduit 638. Heat exchange between the downgoing oxidizing fluid and the upgoing combustion products in the overburden results in enhanced thermal efficiency. A flow of removed combustion products 625 may be balanced with a flow of fuel fluid 621 and oxidizing fluid 623 to maintain a temperature above autoignition temperature but below a temperature sufficient to produce substantial oxides of nitrogen. Also, a constant flow of

AS

fluids may provide a substantially uniform temperature distribution within the oxidation region of inner conduit 638. Outer conduit 636 may be, for example, a stainless steel tube. In this manner, heating of at least the portion of the coal formation may be substantially uniform. As described above, the lower operating temperature may also provide a less expensive metallurgical cost associated with the heating system.

On page 158, please delete the paragraph beginning on line 7, and substitute therefor:

AG

FIG. 40 depicts an embodiment of in situ synthesis gas production integrated with a catalytic methanation process. For example, synthesis gas 1140 exiting production well 1142 may be supplied to catalytic methanation plant 1144. In some embodiments, it may be desirable for the composition of produced synthesis gas, which may be used as a feed gas for a catalytic methanation process, to have a H<sub>2</sub> to carbon monoxide ratio of about three to one. Methane 1146 may be produced by catalytic methanation plant 1144. Steam 1148 produced by plant 1144 may be supplied to injection well 1141 for production of synthesis gas. Examples of a catalytic methanation process are illustrated in U.S. Patent Nos. 3,922,148 to Child; 4,130,575 to Jorn et al.; and 4,133,825 to Stroud et al., which are incorporated by reference as if fully set forth herein.

On page 167, please delete the paragraph beginning on line 8, and substitute therefor:

A7

Alternatively, square patterns may be provided with production wells placed, for example, in the center of each third square, resulting in nine heat sources for each production well. Production wells may be placed within each fifth square in a square pattern, which may result in twenty-five heat sources for each production well.

On page 168, please delete the two paragraphs beginning on line 20, and substitute therefor:

18

FIG. 54 illustrates a pattern of production wells 2760 with inner triangular ring 2766 and outer hexagonal ring 2768. In this pattern, production wells 2760 may be spaced at a distance of 2s. Heat sources 2762 may be located at apices of inner ring 2766 and outer ring 2768. Inner triangular ring 2766 may contribute three equivalent heat sources per production well 2760. Outer hexagonal ring 2768 containing three heater wells may contribute one equivalent heat source per production well 2760. Thus, a total of four equivalent heat sources may provide heat to production well 2760.

FIG. 55 illustrates a pattern of production wells with one inner triangular ring of heat sources surrounding each production well and one irregular hexagonal outer ring. Production wells 2760 may be surrounded by ring 2770 of three heat sources 2762. Production wells 2760 may be spaced at a distance of 3s. Irregular hexagonally shaped ring 2772 of nine heat sources 2762 may surround ring 2770. This pattern may result in a ratio of heat sources 2762 to production wells 2760 of nine.

On page 171, please delete the paragraph beginning on line 16, and substitute therefor:

A9

Power generation unit 2822 may be configured for extracting useable energy from the first portion of stream 2818. For example, stream 2818 may be produced under pressure. In this manner, power generation unit 2822 may include a turbine configured to generate electricity from the first portion of stream 2818. The power generation unit may also include, for example, a molten carbonate fuel cell, a solid oxide fuel cell, or other type of fuel cell. The facilities may be further configured such that the extracted useable energy may be provided to user 2824. User 2824 may include, for example, surface facilities 2800, a heat source disposed within a formation, and/or a consumer of useable energy.

On page 177, please delete the paragraph beginning on line 14, and substitute therefor:

AIO

FIG. 62 illustrates an example of another pattern of heat sources 3000 and production wells 3002. Midlines 3006 are formed equidistant from the two production wells 3002, and perpendicular to a line connecting such production wells. Unit cell 3014 is determined by intersection of midlines 3006 at vertices 3008. Twelve heat sources 3000 are counted in unit cell 3014 by a method as described in the above embodiments, of which six are whole sources of heat, and six are one third sources of heat (with the other two thirds of heat from such six wells going to other patterns). Thus, a ratio of heat sources 3000 to production wells 3002 is determined as 8:1 for the pattern illustrated in FIG. 62. An example of a pattern of heat sources is illustrated in U.S. Patent No. 2,923,535 issued to Ljungstrom, which is incorporated by reference as if fully set forth herein.

On page 187, please delete the paragraph and table title beginning on line 24, and substitute therefor:

AII

Table 1 shows a comparison of gas compositions, in percent volume, obtained from in situ gasification of coal using air injection to heat the coal, in situ gasification of coal using oxygen injection to heat the coal, and in situ gasification of coal in a reducing atmosphere by thermal pyrolysis heating as described in embodiments herein.

#### TABLE 1

On page 188, please delete the paragraph beginning on line 3, and substitute therefor:

AN

As shown in Table 1, gas produced according to an embodiment described herein may be treated and sold through existing natural gas systems. In contrast, gas produced

AIR

by typical in situ gasification processes may not be treated and sold through existing natural gas systems. For example, a heating value of the gas produced by gasification with air was 6000 KJ/m³, and a heating value of gas produced by gasification with oxygen was 11,439 KJ/m³. In contrast, a heating value of the gas produced by thermal conductive heating was 39,159 KJ/m³.

On page 192, please delete the paragraph beginning on line 20, and substitute therefor:

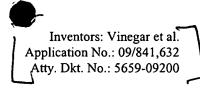
APS

FIG. 97 illustrates a decrease in the assessed thermal conductivity values 3742 at about 100 °C. It is believed that this decrease in thermal conductivity was caused by water vaporizing in the cracks and void spaces (water vapor has a lower thermal conductivity than liquid water). At about 350 °C, the thermal conductivity began to increase, and it increased substantially as the temperature increased to 700 °C. It is believed that the increases in thermal conductivity were the result of molecular changes in the carbon structure. As the carbon was heated it became more graphitic which is illustrated in Table 2 by an increased vitrinite reflectance after pyrolysis. As void spaces increased due to fluid production, heat was increasingly transferred by radiation and/or convection. In addition, concentrations of hydrogen in the void spaces were raised due to pyrolysis and generation of synthesis gas.

On page 194, please delete the paragraph beginning on line 1 (as amended in the Preliminary Amendment), and substitute therefor:

AIA

Hydrocarbon fluids were produced from a portion of a coal formation by an in situ experiment conducted in a portion of a coal formation. The coal was high volatile bituminous C coal. It was heated with electrical heaters. FIG. 98 illustrates a cross-sectional view of the in situ experimental field test system. As shown in FIG. 98, the experimental field test system included coal formation 3802 within the ground and groutwall 3800. Coal formation 3802 dipped at an angle of approximately 36° with a thickness



of approximately 4.9 meters. FIG. 99 illustrates a location of heat sources 3804a, 3804b, 3804c, production wells 3806a, 3806b, and temperature observation wells 3808a, 3808b, 3808c, 3808d used for the experimental field test system. The three heat sources were disposed in a triangular configuration. Production well 3806a was located proximate a center of the heat source pattern and equidistant from each of the heat sources. A second production well 3806b was located outside the heat source pattern and spaced equidistant from the two closest heat sources. Grout wall 3800 was formed around the heat source pattern and the production wells. The grout wall was formed of 24 pillars. Grout wall 3800 was configured to inhibit an influx of water into the portion during the in situ experiment. In addition, grout wall 3800 was configured to substantially inhibit loss of

On page 195, please delete the paragraph and table title beginning on line 14, and substitute therefor:

generated hydrocarbon fluids to an unheated portion of the formation.

Table 2 illustrates the results from analyzing coal before and after it was treated (including heating the temperatures set forth in as is set forth in FIG. 101 (i.e., after pyrolysis and production of synthesis gas) as described above. The coal was cored at about 11-11.3 meters from the surface, midway into the coal bed, in both the "before treatment" and "after treatment" examples. Both cores were taken at about the same location. Both cores were taken at about 0.66 meters from well 3804c (between the grout wall and well 3804c) in FIG. 99. In the following Table 2 "FA" means Fisher Assay, "as rec'd" means the sample was tested as it was received and without any further treatment, "Py-Water" means the water produced during pyrolysis, "H/C Atomic Ratio" means the atomic ratio of hydrogen to carbon, "daf" means "dry ash free," "dmmf" means "dry mineral matter free," and "mmf" means "mineral matter free." The specific gravity of the "after treatment" core sample was approximately 0.85 whereas the specific gravity of the "before treatment" core sample was approximately 1.35.

TABLE 2

1

On page 196, please delete the two paragraphs beginning on line 3, and substitute therefor:

A16

À.

Even though the cores were taken outside the areas within the triangle formed by the three heaters in FIG. 99, nevertheless the cores demonstrate that the coal remaining in the formation changed significantly during treatment. The vitrinite reflectance results shown in Table 2 demonstrate that the rank of the coal remaining in the formation changed substantially during treatment. The coal was a high volatile bituminous C coal before treatment. After treatment, however, the coal was essentially anthracite. The Fischer Assay results shown in Table 2 demonstrate that most of the hydrocarbons in the coal had been removed during treatment. The H/C Atomic Ratio demonstrates that most of the hydrogen in the coal had been removed during treatment. A significant amount of nitrogen and ash was left in the formation.

In sum, the results shown in Table 2 demonstrate that a significant amount of hydrocarbons and hydrogen were removed during treatment of the coal by pyrolysis and generation of synthesis gas. Significant amounts of undesirable products (ash and nitrogen) remain in the formation, while the significant amounts of desirable products (e.g., condensable hydrocarbons and gas) were removed.

On page 199, please delete the paragraph beginning on line 26, and substitute therefor:



An experiment was conducted on the coal formation treated according to the in situ conversion process to measure the uniform permeability of the formation after pyrolysis. After heating a portion of the coal formation, a ten minute pulse of CO<sub>2</sub> was injected into the formation at first production well 3806a and produced at well 3804a, as shown in FIG. 99. The CO<sub>2</sub> tracer test was repeated from production well 3806a to well 3804b and from production well 3806a to well 3804c. As described above, each of the

three different heat sources were located equidistant from the production well. The CO<sub>2</sub> was injected at a rate of 4.08 m<sup>3</sup>/h (144 standard cubic feet per hour). As illustrated in FIG. 109, the CO<sub>2</sub> reached each of the three different heat sources at approximately the same time. Line 3900 illustrates production of CO<sub>2</sub> at heat source 3804a, line 3902 illustrates production of CO<sub>2</sub> at heat source 3804b, and line 3904 illustrates production of CO<sub>2</sub> at heat source 3804c. As shown in FIG. 111, yield of CO<sub>2</sub> 3910 from each of the three different wells was also approximately equal over time. Such approximately equivalent transfer of a tracer pulse of CO<sub>2</sub> through the formation and yield of CO<sub>2</sub> from the formation indicated that the formation was substantially uniformly permeable. The fact that the first CO<sub>2</sub> arrival only occurs approximately 18 minutes after start of the CO<sub>2</sub> pulse indicates that no preferential paths had been created between well 3806a and wells 3804a, 3804b, and 3804c.

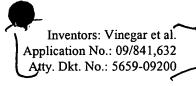
On page 201, please delete the paragraph beginning on line 19, and substitute therefor:

From FIG. 113, the maximum natural water inflow is approximately 5 kg/h as indicated by arrow 3920. Arrows 3922, 3924, and 3926 represent injected water rates of about 2.7 kg/h, 5.4 kg/h, and 11 kg/h, respectively, into central well 3806a of FIG. 99. Production of synthesis gas is at heater wells 3804a, 3804b, and 3804c. FIG. 113 shows that the synthesis gas production per unit volume of water injected decreases at arrow 3922 at approximately 2.7 kg/h of injected water or 7.7 kg/h of total water inflow. The reason for the decrease is that steam is flowing too fast through the coal seam to allow the reactions to approach equilibrium conditions.

On page 204, please delete the paragraph and table title beginning on line 10, and substitute therefor:

٠.,

Table 3 includes a composition of synthesis gas produced during a run of the in situ coal field experiment.



A19

### TABLE 3

On page 205, please delete the paragraph beginning on line 26 (as amended in the Preliminary Amendment), and substitute therefor:

420

•

FIG. 122 is a plot of calculated equilibrium wet mole fractions for a coal reaction with water. Equilibrium wet mole fractions are shown for water 4006, H<sub>2</sub> 4008, carbon monoxide 4010, and carbon dioxide 4012 as a function of temperature at a pressure of 2 bars absolute. At 390 °C, the produced gas includes about 89 % water, about 7 % H<sub>2</sub>, and about 4 % carbon dioxide. At 500 °C, the produced gas includes about 66 % water, about 22 % H<sub>2</sub>, about 11 % carbon dioxide, and about 1 % carbon monoxide. At 700 °C, the produced gas includes about 18 % water, about 47.5 % H<sub>2</sub>, about 12 % carbon dioxide, and about 22.5 % carbon monoxide.

On page 207, please delete the paragraph beginning on line 1 (as amended in the Preliminary Amendment), and substitute therefor:

AUS.

In the embodiments of FIG. 123, the methane reactions in Equations (4) and (5) are included. The calculations set forth herein assume that char is only made of carbon and that there is an excess of carbon to steam. About 890 MW of energy 4024 is required to pyrolyze about 105,800 metric tons per day of coal. The pyrolysis products 4028 include liquids and gases with a production of 23,000 cubic meters per day. The pyrolysis process also produces about 7,160 metric tons per day of water 4030. In the synthesis gas stage about 57,800 metric tons per day of char with injection of 23,000 metric tons per day of steam 4032 and 2,000 MW of energy 4034 with a 20% conversion will produce 12,700 cubic meters equivalent oil per day of synthesis gas 4038.

On page 209, please delete the paragraph and table title beginning on line 15, and substitute therefor:

AZZ

Table 4 is an overview of the potential production volume of applications of synthesis gas produced by wet oxidation. The estimates are based on 56.6 million standard cubic meters of synthesis gas produced per day at 700 °C.

#### TABLE 4

Op page 210, please delete the paragraph and table title beginning on line 26, and substitute therefor:

Ars

**'**、;

Computer simulations have demonstrated that carbon dioxide may be sequestered in both a deep coal formation and a post treatment coal formation. The Comet2 Simulator determined the amount of carbon dioxide that could be sequestered in a San Juan Basin type deep coal formation and a post treatment coal formation. The simulator also determined the amount of methane produced from the San Juan Basin type deep coal formation due to the carbon dioxide injection. The model employed for both the deep coal formation and the post treatment coal formation was a 1.3 km² area, with a repeating 5 spot well pattern. The 5 spot well pattern included four injection wells arranged in a square and one production well at the center of the square. The properties of the San Juan Basin and the post treatment coal formations are shown in Table 5. Additional details of simulations of carbon dioxide sequestration in deep coal formations and comparisons with field test results may be found in *Pilot Test Demonstrates How Carbon Dioxide Enhances Coal Bed Methane Recovery*, Lanny Schoeling and Michael McGovern, Petroleum Technology Digest, Sept. 2000, p. 14-15.

## TABLE 5

On page 213, please delete the paragraph beginning on line 2, and substitute therefor:

AZA

FIG. 130 illustrates the pressure at the wellhead of the injection wells as a function of time during the simulation. The pressure decreased from about 114 bars absolute to about 19 bars absolute over the first 370 days. The decrease in the pressure was due to removal of water from the coal formation. Pressure then started to increase substantially as carbon dioxide injection started at 370 days. The pressure reached a maximum of about 98 bars absolute. The pressure then began to gradually decrease after 480 days. At about 1440 days, the pressure increased again to about 98 bars absolute due to the increase in the carbon dioxide injection rate. The pressure gradually increased until about 3640 days. The pressure jumped at about 3640 days because the production well was closed off.

On page 214, please delete the paragraph beginning on line 10, and substitute therefor:



Table 5 shows that the permeability and porosity of the simulation in the post treatment coal formation were both significantly higher than in the deep coal formation prior to treatment. Also, the initial pressure was much lower. The depth of the post treatment coal formation was shallower than the deep coal bed methane formation. The same relative permeability data and PVT data used for the deep coal formation were used for the coal formation simulation. The initial water saturation for the post treatment coal formation was set at 70 %. Water was present because it is used to cool the hot spent coal formation to 25 °C. The amount of methane initially stored in the post treatment coal is very low.

# In the Claims:

Listed below is a copy of amended claims 4515, 4550, 4551, 4552, 4554, and 4555. A marked-up copy of these claims is provided in an accompanying document. The amendments correct typographical errors.

FIG. 130 illustrates the pressure at the wellhead of the injection wells as a function of time during the simulation. The pressure decreased from about 114 bars absolute to about 19 bars absolute over the first 370 days. The decrease in the pressure was due to removal of water from the coal formation. Pressure then started to increase substantially as carbon dioxide injection started at 370 days. The pressure reached a maximum of about 98 bars absolute. The pressure then began to gradually decrease after 480 days. At about 1440 days, the pressure increased again to about 98 bars absolute due to the increase in the carbon dioxide injection rate. The pressure gradually increased until about 3640 days. The pressure jumped at about 3640 days because the production well was closed off.

On page 214, please delete the paragraph beginning on line 10, and substitute therefor:

Table 5 shows that the permeability and porosity of the simulation in the post treatment coal formation were both significantly higher than in the deep coal formation prior to treatment. Also, the initial pressure was much lower. The depth of the post treatment coal formation was shallower than the deep coal bed methane formation. The same relative permeability data and PVT data used for the deep coal formation were used for the coal formation simulation. The initial water saturation for the post treatment coal formation was set at 70 %. Water was present because it is used to cool the hot spent coal formation to 25 °C. The amount of methane initially stored in the post treatment coal is very low.

### In the Claims:

Listed below is a copy of amended claims 4550, 4551, 4552, 4554, and 4555. A marked-up copy of these claims is provided in an accompanying document. The amendments correct typographical errors.